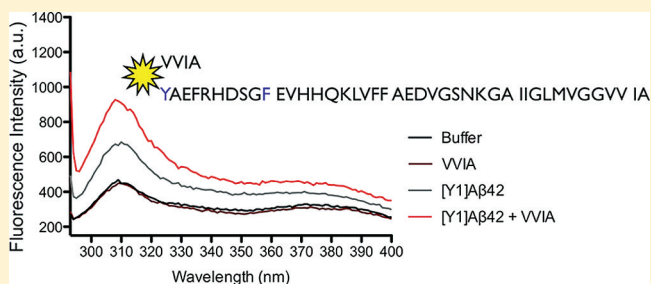


C-Terminal Tetrapeptides Inhibit A β 42-Induced Neurotoxicity Primarily through Specific Interaction at the N-Terminus of A β 42Huiyuan Li,[†] Zhenming Du,^{||} Dahabada H. J. Lopes,[†] Erica A. Fradinger,^{†,⊥} Chunyu Wang,^{||} and Gal Bitan^{*,†,‡,§}[†]Department of Neurology, David Geffen School of Medicine, [‡]Brain Research Institute, and [§]Molecular Biology Institute, University of California, Los Angeles, 635 Charles E. Young Drive South, Los Angeles, California 90095-7334, United States^{||}Department of Biology, Rensselaer Polytechnic Institute, 110 Eighth Street, Troy, New York 12180, United States

S Supporting Information

ABSTRACT: Inhibition of amyloid β -protein (A β)-induced toxicity is a promising therapeutic strategy for Alzheimer's disease (AD). Previously, we reported that the C-terminal tetrapeptide A β (39–42) is a potent inhibitor of neurotoxicity caused by A β 42, the form of A β most closely associated with AD. Here, initial structure–activity relationship studies identified key structural requirements, including chirality, side-chain structure, and a free N-terminus, which control A β (39–42) inhibitory activity. To elucidate the binding site(s) of A β (39–42) on A β 42, we used intrinsic tyrosine (Y) fluorescence and solution-state NMR. The data suggest that A β (39–42) binds at several sites, of which the predominant one is located in the N-terminus of A β 42, in agreement with recent modeling predictions. Thus, despite the small size of A β (39–42) and the hydrophobic, aliphatic nature of all four side-chains, the interaction of A β (39–42) with A β 42 is controlled by specific intermolecular contacts requiring a combination of hydrophobic and electrostatic interactions and a particular stereochemistry.



■ INTRODUCTION

Neurotoxic oligomers of amyloid β -protein (A β) are believed to be the main cause of Alzheimer's disease (AD).^{1–4} Two predominant forms of A β , comprising 40 (A β 40) or 42 (A β 42) amino acid residues, are produced in vivo. A β 42 has been shown to be more neurotoxic than A β 40⁵ and to follow a different pathway of oligomerization.^{6,7} A β 42 forms higher-order metastable oligomers than A β 40, and this tendency correlates with structural stabilization of the C-terminus of A β 42 mediated by the presence of I41 and A42.^{6,8–10}

Inhibition of A β aggregation by short peptides derived from the sequence of A β itself has been used by a number of groups, primarily along the idea of “ β -sheet breaker” peptides that interfere with formation of the characteristic β -sheet-rich amyloid fibrils. The most utilized sequence for this line of investigation has been the central hydrophobic cluster of A β (CHC, residues 17–21),^{11–16} which is a key region in A β fibrillogenesis.¹⁷ Utilizing a similar strategy, recently, rationally designed aminopyrazole-based β -sheet breakers were found to inhibit A β assembly and toxicity, with the most effective inhibitor being a conjugate of aminopyrazole and the CHC-derived sequence LPFFD.¹⁸ Using a different A β region for inhibitor design, modified A β 42 C-terminal fragments, GVVIA-NH₂ and RVVIA-NH₂, were designed as β -sheet breakers and partially protected SH-SY5Y neuroblastoma cells from A β 42 neurotoxicity in cell viability¹⁹ but not electrophysiological assays.²⁰ In a different study, hexapeptides derived from

A β (32–37) with varying extent of N-methylation were found to retard β -sheet and fibril formation and reduce A β neurotoxicity.²¹

As evidence emerged ascribing pathogenic primacy to A β oligomers rather than fibrils,²² inhibitor-design efforts have shifted toward inhibition of A β oligomerization. Guided by the principle of self-recognition and considering the critical role of the C-terminal region of A β 42 in self-assembly,^{6,8} we prepared C-terminal fragments (CTFs) of the general formula A β (x –42), x = 28–39, and evaluated their capability to disrupt the assembly and neurotoxicity of A β 42.²³ Of the 12 CTFs tested, the shortest one, A β (39–42), had surprisingly high activity. A β (39–42) was found to inhibit A β 42-induced neurotoxicity in differentiated rat pheochromocytoma (PC-12) cells with half-maximal (IC₅₀) values of 16 ± 5 and 47 ± 14 μ M using the (3-(4,5-dimethylthiazol-2-yl)-2,5-diphenyltetrazolium bromide (MTT) reduction and lactate dehydrogenase (LDH) release assays, respectively.²³ In addition, A β (39–42) significantly rescued mouse primary hippocampal neurons from A β 42-induced inhibition of miniature excitatory postsynaptic current frequency.²³ The data suggested that A β (39–42) inhibited A β 42-induced toxicity both in the early stage of synaptic activity and in later stages of metabolism deficits and cell death.

Received: July 22, 2011

Published: November 16, 2011

In follow-up dynamic light scattering studies, we found that $A\beta(39-42)$ stabilized oligomers with a hydrodynamic radius of 6 ± 3 nm and 30 ± 10 nm, which we interpreted as resulting from formation of heterooligomers comprising both $A\beta42$ and $A\beta(39-42)$.^{23,24} Computer modeling of $A\beta(39-42)$ co-assembled with $A\beta42$ supported the formation of heterooligomers and suggested that $A\beta(39-42)$ binds near the N-terminal region, $A\beta(2-4)$, and sequesters this region from the aqueous milieu.^{23,25}

The amphipathic nature and small size of $A\beta(39-42)$ make its pharmacokinetic characteristics close to recommended values of drug-like criteria, including Lipinski's Rule of 5²⁶ and topological polar surface area (tPSA)²⁷ (Table 1),

Table 1. Physicochemical Characteristics of $A\beta(39-42)$

criterion	recommended value	
	Lipinski's rule of 5 ²⁶	$A\beta(39-42)$
MW	<500	400.5
ClogP	<5	-0.3
H-bond donors	≤ 5	5
H-bond acceptors	≤ 10	9
tPSA (\AA^2)	≤ 140 ²⁷	150.62

supporting its development as a drug lead. Toward this end, here we performed structure-activity relationship (SAR) studies to delineate structural features important for inhibitory activity and characterized the binding of $A\beta(39-42)$ to $A\beta42$ using intrinsic fluorescence and two-dimensional (2D) solution-state NMR. The data suggest that $A\beta(39-42)$ protects cells against $A\beta42$ -induced toxicity predominantly via specific interaction at the N-terminus of $A\beta42$.

RESULTS

Structure-Activity Relationship Study of $A\beta(39-42)$.

To guide future rational development of $A\beta(39-42)$ as a drug lead, we asked what structural characteristics were important for the inhibitory activity and what specific interactions controlled the binding of $A\beta(39-42)$ to $A\beta42$. In search of the answers for these questions, we synthesized a series of $A\beta(39-42)$ derivatives, including A substitution of the first three residues (AVIA, VAIA, VVAA), an inversed-peptide (vvia, lower-case letters represent D-configuration), the N-terminally and C-terminally protected analogues Ac-VVIA, VVIA-NH₂, a retro-peptide (AIVV), and N-terminally and C-terminally protected versions of the retro-peptide (Ac-AIVV, AIVV-NH₂) (Table 2).

We began evaluating the new derivatives by testing if these peptides themselves were toxic to differentiated PC-12 cells using the MTT assay. The results showed that all the derivatives were not toxic (Figure 1, white bars). Notably, $A\beta(39-42)$ and the analogues, AVIA, VAIA, VVIA-NH₂, AIVV, and AIVV-NH₂ caused a significant increase of 10–35% in cell viability relative to control cells.

Next, we screened the $A\beta(39-42)$ derivatives for inhibition of $A\beta42$ -induced neurotoxicity in single-dose experiments. Differentiated PC-12 cells were incubated with $A\beta42$ for 24 h in the absence or presence of 10-fold excess of each derivative, and cell viability was assessed using the MTT assay. Among the nine derivatives tested, the same five analogues that increased cell viability on their own showed statistically significant attenuation of $A\beta42$ -induced toxicity (Figure 1, black bars), similar to the parent peptide. The A-substituted sequences, AVIA and VAIA, showed similar inhibitory activity to that of

Table 2. Sequences, Masses, and IC₅₀ Values of $A\beta(39-42)$ and Derivatives

sequence	calculated mass [M + H]	observed mass	IC ₅₀ (μM) (MTT)	IC ₅₀ (μM) (LDH)
VVIA	401.5	401.2	21 ± 6	16 ± 3
AVIA	373.5	373.0	53 ± 10	22 ± 5
VAIA	373.5	373.2	15 ± 3	14 ± 2
VVAA	359.4	359.1	nd	nd
vvia ^a	401.5	401.2	nd	nd
Ac-VVIA	443.6	443.4	nd	nd
VVIA-NH ₂	400.5	400.1	28 ± 7	30 ± 5
AIVV	401.5	401.3	14 ± 1	22 ± 3
Ac-AIVV	443.5	443.1	nd	nd
AIVV-NH ₂	400.5	400.2	20 ± 4	16 ± 3

^aLower-case letters represent D-configuration. nd: not determined.

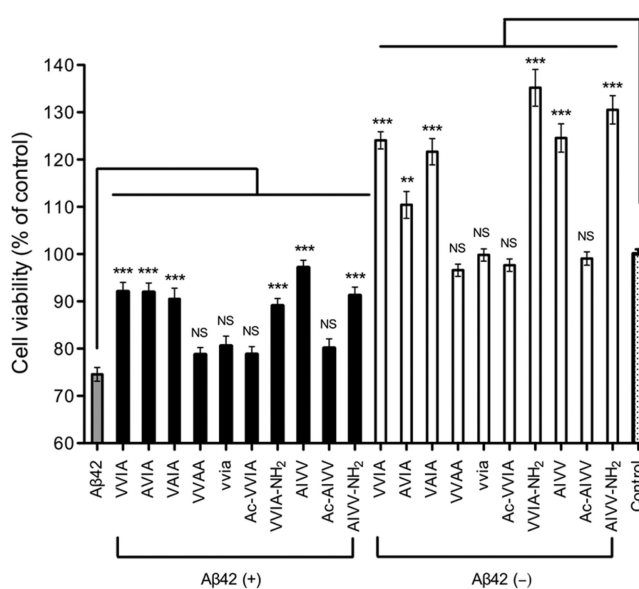


Figure 1. Evaluation of inhibitory activity of $A\beta(39-42)$ analogues. $A\beta42$ ($10 \mu\text{M}$, gray bar), mixtures of $A\beta42:A\beta(39-42)$ analogues at 1:10 concentration ratio (black bars), $A\beta(39-42)$ analogues alone at $100 \mu\text{M}$ (white bars), or control medium containing NaOH at the same concentration as in the peptide solutions (dotted bar) were incubated with differentiated PC-12 cells for 24 h and cell viability was measured using the MTT assay. The data are shown as mean \pm SEM of at least three independent experiments with six replicates per data point ($n \geq 18$). Statistical significance was calculated and compared with $A\beta42$ alone by using ANOVA followed by Dennett's multiple-comparison tests (** $p < 0.01$, *** $p < 0.001$), NS = non-significant.

$A\beta(39-42)$, whereas VVAA lost inhibitory activity suggesting that the side-chains of V39 (full-length $A\beta$ numbering) and V40 were relatively insensitive to structural changes, but the side-chain of I41 was important for inhibition. However, the observation that inhibitory activity was maintained in the retro sequence, AIVV, suggested that a bulky hydrophobic side-chain in position 41, such as I or V, might be sufficient for the inhibitory activity. The loss of activity in the inversed-peptide (vvia) indicated that the chirality of $A\beta(39-42)$ was required for inhibition of toxicity. The analogues in which the N-terminus was acetylated, Ac-VVIA and Ac-AIVV, showed no inhibitory activity, whereas the analogues with amidated C-terminus, VVIA-NH₂ and AIVV-NH₂, were as active as $A\beta(39-42)$.

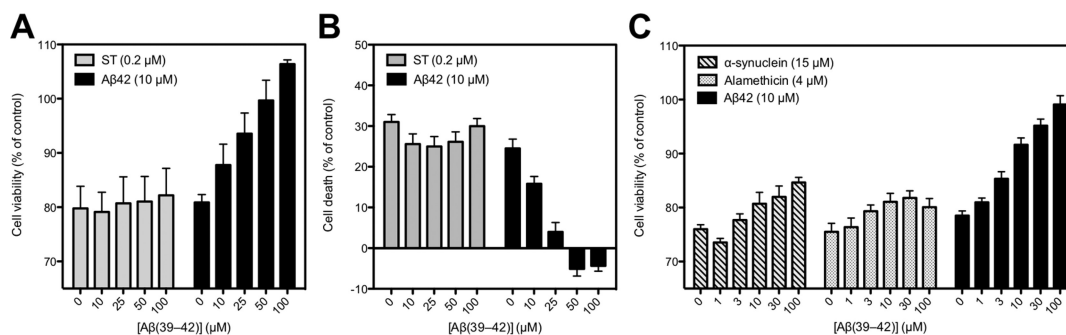


Figure 2. $A\beta(39-42)$ selectively inhibits $A\beta42$ -induced toxicity. $A\beta42$ ($10 \mu\text{M}$) or staurosporine (ST, $0.2 \mu\text{M}$) in the absence or presence of different $A\beta(39-42)$ concentrations were (A) incubated with differentiated PC-12 cells for 24 h and cell viability was determined using MTT assay, and (B) incubated with differentiated PC-12 cells for 48 h and cell death was measured using LDH assay. (C) α -Synuclein ($15 \mu\text{M}$), alamethicin ($4 \mu\text{M}$), or $A\beta42$ ($10 \mu\text{M}$) in the absence or presence of different $A\beta(39-42)$ concentrations were incubated with differentiated PC-12 cells for 24 h, and viability was determined using MTT assay. The data represent mean \pm SEM from at least three independent experiments with five replicates per data point ($n \geq 15$).

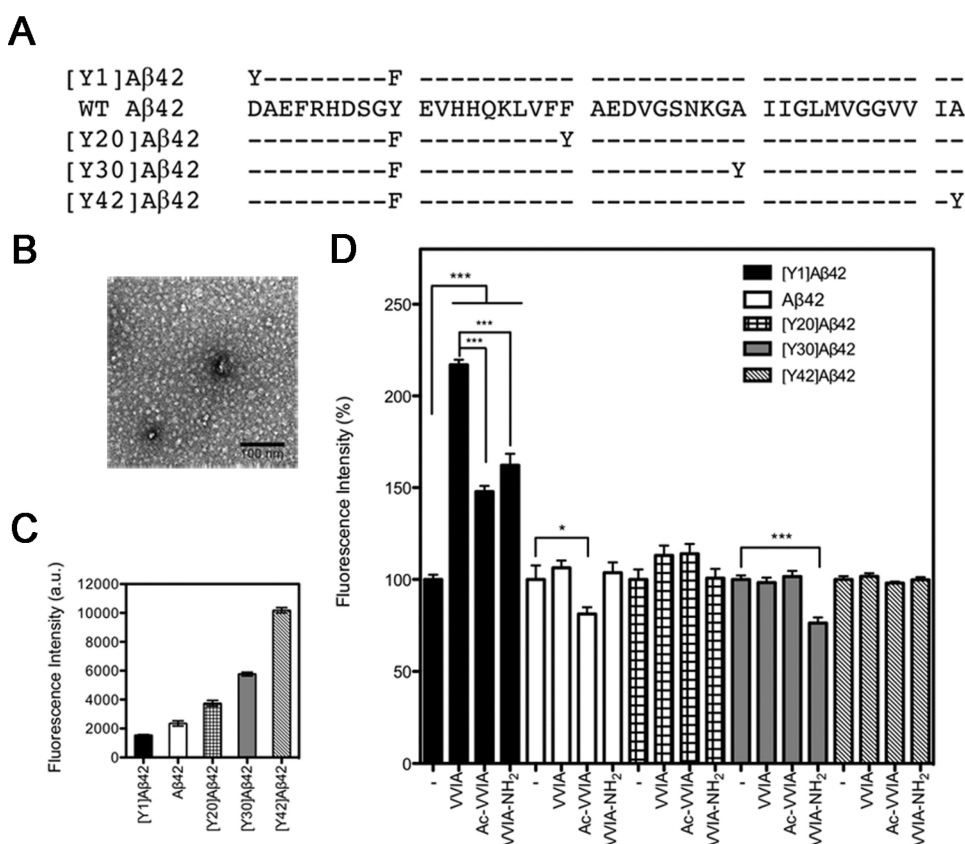


Figure 3. Intrinsic fluorescence of $A\beta42$ analogues in the presence of $A\beta(39-42)$ or its derivatives. (A) Primary structure of $A\beta42$ and its Y-substituted analogues. Hyphens indicate residues identical to WT $A\beta42$. In WT $A\beta42$, Y is at position 10. The substitutions, in which a single Y residue substituted the original residues at positions (n) 1, 20, 30, or 42, and the native Y10 was substituted by F, are simply named $[Y_n]A\beta42$. (B) Representative electron micrograph of freshly prepared $5 \mu\text{M}$ $A\beta42$. The scale bar represents 100 nm. (C) Intrinsic fluorescence intensity of $5 \mu\text{M}$ $A\beta42$ and each Y-substituted analogue. (D) Intrinsic fluorescence of $A\beta42$ analogues in the presence of $A\beta(39-42)$, Ac-VVIA, or VVIA-NH₂ normalized to the percentage of each $A\beta42$ analogue alone. The data are shown as mean \pm SEM of four independent experiments with at least 10 measurements per data point. Statistical significance was analyzed using ANOVA followed by Bonferroni's and Dennett's multiple-comparison tests ($*p < 0.05$, $***p < 0.001$).

42), indicating that a free N-terminal amino group was essential for the activity, whereas the C-terminus could be modified to provide protection from carboxypeptidases.

Further characterization showed that all the active derivatives inhibited $A\beta42$ -induced toxicity dose-dependently (Table 2 and Supporting Information Figure S1). The differences among the IC₅₀ values of the $A\beta(39-42)$ derivatives in the MTT assay

were relatively small and not statistically significant, except for the IC₅₀ of AVIA, $53 \pm 10 \mu\text{M}$, which was significantly higher ($p = 0.0081$, Student's t test) than that of $A\beta(39-42)$, $21 \pm 6 \mu\text{M}$. The differences among the IC₅₀ values found in the LDH assay for all the $A\beta(39-42)$ derivatives were statistically insignificant.

A β (39–42) Specifically Inhibits A β 42-Induced Toxicity. Because A β (39–42) and some of its analogues caused increased cell viability relative to cells treated with cell culture medium alone, we asked whether the observed inhibition of A β 42-induced toxicity was mediated, at least partially, by a mechanism that did not involve interaction with A β 42. To address this question, we compared the effect of A β (39–42) on neurotoxicity induced by A β 42 and several other toxins. For initial examination we used staurosporine, a nonselective protein-kinase inhibitor that induces apoptosis in multiple cell types.²⁸ Differentiated PC-12 cells treated with 0.2 μ M staurosporine or 10 μ M A β 42 showed similar decrease in cell viability in both the MTT (Figure 2A) and the LDH (Figure 2B) assays. As expected, A β (39–42) showed dose-dependent inhibition of A β 42-induced toxicity. In contrast, A β (39–42) had no effect on staurosporine-induced cell death.

One mechanism by which A β 42 is thought to cause toxicity is disruption of the cell membrane leading to leakage of ions and/or other metabolites, either due to formation of non-specific channels²⁹ or via perturbation of the phospholipid bilayer conductance without channel formation.³⁰ To examine whether A β (39–42) protected the cells against membrane perturbation, we examined next its ability to protect against alamethicin, a fungal peptide antibiotic, which potently induces voltage-dependent ion channel formation in phospholipid membranes.³¹ In addition, we used another amyloidogenic protein, α -synuclein, for which similar mechanisms of toxicity to A β 42 have been proposed.³² Differentiated PC-12 cells treated with 15 μ M α -synuclein, 4 μ M alamethicin, or 10 μ M A β 42 showed similar decrease in cell viability in MTT assay (Figure 2C). Addition of increasing concentrations of A β (39–42) resulted in dose-dependent inhibition of the toxicity induced by A β 42, as observed in previous experiments (Figure 2A and Supporting Information Figure S1). In contrast, only weak protection from α -synuclein- or alamethicin-induced toxicity was observed, suggesting that nonspecific protection was a minor component of the inhibitory effect of A β (39–42), whereas the major mechanism was mediated through direct and specific interaction with A β 42.

Binding Site(s) of A β (39–42) on A β 42. Originally, the hypothesis that led us to examine A β 42 CTFs as inhibitors of A β 42 assembly and toxicity was based on the principle of self-recognition and we predicted that the CTFs would bind to the C-terminus of A β 42.^{23,33} However, our previous investigation of the mode of interaction between the CTFs and A β 42 suggested that different CTFs might inhibit A β 42-induced toxicity by distinct mechanisms^{23,24} and might bind A β 42 at sites other than the C-terminus.²⁵ Therefore, here we used two complementary methods to elucidate the binding site(s) of A β (39–42), the shortest CTF in original series, on A β 42.

Characterization of the Interaction between A β (39–42) and A β 42 by Intrinsic Y Fluorescence. Elucidation of binding sites for inhibitors of aberrant protein self-assembly is a difficult task because the self-assembly typically occurs among disordered monomers and produces metastable oligomers in which the degree of order still is low. To explore potential binding site(s) of A β (39–42) on A β 42, we took advantage of the intrinsic fluorescence of Y residues, which enables rapid signal detection at low concentrations under which minimal or no aggregation occurs during the time of the experiment (\sim 30 min), thus measuring binding to monomers and low-order oligomers.

In addition to wild-type (WT) A β 42, in which a single Y residue is at position 10, we used analogues in which Y substituted the original residues at positions 1, 20, 30, or 42, and the native Y10 was substituted by the fluorometrically silent F. The sequences of WT A β 42 and its Y-substituted analogues are shown in Figure 3A. These analogues were used previously to study A β 42 folding and assembly.^{34,35} Morphological studies by electron microscopy (EM) showed that all the Y-substituted A β 42 analogues formed fibrils, and the fibril morphologies observed were similar to those formed by WT A β 42.³⁴ Secondary structure dynamics examination by circular dichroism spectroscopy showed that qualitatively all the Y-substituted analogues were predominately disordered initially and then displayed characteristic statistical coil to α -helix to β -sheet transitions during oligomerization and fibril formation.³⁴

Exposure to the aqueous milieu is known to decrease Y fluorescence intensity without altering the wavelength of maximum emission (λ_{max}). In addition, the fluorescence of the phenol group in the Y side-chain can be quenched by exposure to hydrated carbonyl groups or through hydrogen-bond formation with peptide carbonyls or with carboxylate groups in aspartate or glutamate side-chains.^{34,36} In our experimental system, an increase in Y fluorescence upon addition of A β (39–42) would suggest a decrease in solvent exposure, possibly indicating binding of the tetrapeptide to, or in the vicinity of, the Y residue. Alternatively, an increase in fluorescence could be interpreted as arising from increase in intra- or intermolecular interactions within or between A β 42 monomers, respectively. However, we reasoned that changes in fluorescence resulting from global folding and/or assembly of A β 42 likely would affect Y residues in multiple positions, whereas specific, local binding of A β (39–42) would lead to increased Y fluorescence only in a specific position.

To minimize A β aggregation during the assay, all the samples were pretreated with 1,1,1,3,3,3-hexafluoroisopropanol (HFIP),^{37,38} and measurement of fluorescence was initiated immediately following rehydration. In addition, aliquots were monitored by EM. During the time of fluorescence measurements (\sim 30 min), all the peptides formed quasiglobular structures with diameters ranging from \sim 7 to 15 nm and no fibrils were observed. A representative electron micrograph of A β 42 prepared under these conditions is shown in Figure 3B. The fluorescence intensity of A β 42 and its Y-substituted analogues is shown in Figure 3C. Consistent with a previous report,³⁴ the observed trend suggested that the degree of exposure to the aqueous solvent decreased gradually from the N- to the C-terminus.

The fluorescence intensity of A β 42 analogues (5 μ M) mixed with A β (39–42) (50 μ M) is shown in the second bar of each group in Figure 3D. To facilitate the comparison among the five A β 42 analogues, the fluorescence intensity in the presence of A β (39–42) in each case was normalized to the fluorescence of the analogue in the absence of A β (39–42) (first bar of each group in Figure 3D). We found that upon addition of A β (39–42), the fluorescence of [Y1]A β 42 increased by $117 \pm 3\%$. In contrast, the fluorescence of WT A β 42, [Y20]A β 42, [Y30]A β 42, and [Y42]A β 42 did not change significantly upon addition of A β (39–42). These results suggested that A β (39–42) bound mainly at the N-terminus of A β 42.

Because the N-terminus of A β contains several charged residues, we hypothesized that the charged amino and carboxyl groups in A β (39–42) might be important for its binding to the N-terminus of A β 42. To test this hypothesis, we examined the

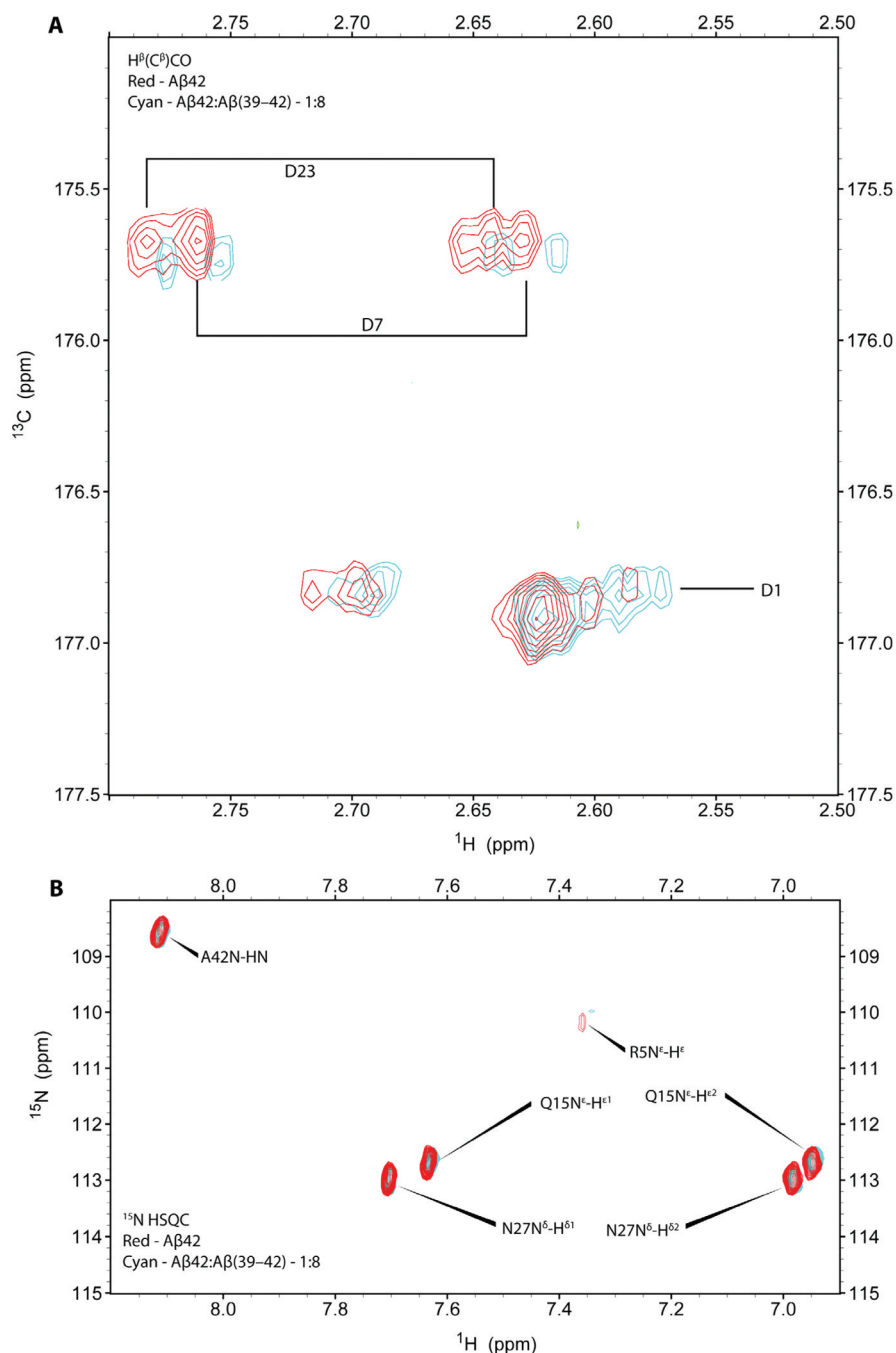


Figure 4. $A\beta(39-42)$ binding site on $A\beta42$ determined by solution-state 2D NMR. $A\beta42$ resonances were measured in the absence (red) or presence (cyan) of 8-fold excess $A\beta(39-42)$. (A) 2D $^{13}\text{C}-^1\text{H}$ HSQC spectrum of $A\beta42$ in the absence or presence of $A\beta(39-42)$ at 4 °C. $\text{H}^\beta(\text{C}^\beta)\text{CO}$ experiments detected upfield movement and reduced intensity of chemical shifts for the side-chains of D1, D7, and D23 upon addition of $A\beta(39-42)$. (B) 2D $^{15}\text{N}-^1\text{H}$ HSQC spectra of $A\beta42$ in the absence or presence of $A\beta(39-42)$ detected upfield movement and reduced intensity of chemical shifts for the $\text{N}^\epsilon\text{-H}^\epsilon$ crosspeak of R5.

effect of $A\beta(39-42)$ analogues in which the N- or C-termini were blocked by acetylation (Ac-VVIA) or amidation (VVIA-NH₂), respectively, on Y fluorescence of $A\beta42$ and its Y-substituted analogues. Representative spectra are shown in Supporting Information Figure S2. The results are shown in the third and fourth bars of each group in Figure 3D, respectively. Upon addition of Ac-VVIA or VVIA-NH₂, the fluorescence of [Y1] $A\beta42$ increased by $48 \pm 3\%$ and $62 \pm 6\%$, respectively. These values were 2.4- and 1.8-times lower than with unmodified $A\beta(39-42)$, suggesting that both the carboxyl and amino groups of $A\beta(39-42)$ contributed to the interaction

with $A\beta42$. The larger loss of affinity caused by blocking the N-terminus relative to blocking the C-terminus of $A\beta(39-42)$ is consistent with the loss of inhibitory activity observed for the N-terminally acetylated analogue (Figure 1). Small effects on fluorescence were observed in two other positions. The fluorescence of $A\beta42$ decreased by $19 \pm 3\%$ upon addition of Ac-VVIA, and the fluorescence of [Y30] $A\beta42$ decreased by $24 \pm 3\%$ upon addition of VVIA-NH₂. These data suggested that removing either one of the charges in $A\beta(39-42)$ decreased the affinity of the peptide for the putative $A\beta42$ N-terminal binding site and increased affinity for alternative binding sites.

Analysis of the interaction of other A β (39–42) analogues with [Y1]A β 42 using internal Y fluorescence showed that the fluorescence increase induced by the N-terminally acetylated and C-terminally amidated retro sequences (Ac-AIVV and AIVV-NH₂), and by the inverso-peptide (vvia) also were significantly lower than those of A β (39–42) (Supporting Information Figure S3), in agreement with the low inhibitory activity of these analogues. Not all the fluorescence results correlated directly with the inhibition data presented in Figure 1, presumably because small sequence perturbation might affect the binding mode of the tetrapeptide derivatives. Exploring the binding sites of all the derivatives was beyond the scope of this study, which was limited to delineation of the major binding sites of the lead compound and the effect of the structural changes that were found to have the greatest effect on the inhibitory activity, namely the charge and chirality in A β (39–42) analogues, which also had the greatest effect on binding to the N-terminal region of A β 42.

Solution-State NMR Characterization of the Interaction between A β (39–42) and A β 42. To complement the intrinsic fluorescence experiments, we used solution-state, ¹⁵N–¹H and ¹³C–¹H heteronuclear single quantum coherence (HSQC) NMR experiments, which enable detection of residue-specific signal perturbation upon binding of unlabeled A β (39–42) to ¹⁵N- or ¹³C/¹⁵N-labeled A β 42. In preliminary experiments, the NMR signal was observed to decrease gradually over 24 h due to self-assembly of A β 42, as reported previously.³⁹ Nonetheless, during the relatively short time needed for acquiring HSQC spectra (~37 min), perturbation of specific resonances upon addition of A β (39–42) could be observed.

The chemical shifts of most of the amino acid residues in A β 42 remained unchanged in the presence of 8-fold molar excess A β (39–42) with the exceptions of small changes in D and R side chains. 2D H ^{β} (C ^{β})CO experiments optimized to detect D side chains were collected to identify and monitor the interaction of these side chains with A β (39–42). As shown in Figure 4A, the ¹H/¹³C signal of the D7 and D23 side-chains showed a small shift and decreased in intensity upon addition of A β (39–42) to A β 42. The resonances for the D1 side chain were isolated from D7 and D23 side-chain resonances and appeared as multiple cross-peaks likely due to slow chemical exchange. The side-chain resonance of R5 also was perturbed upon addition of A β (39–42) to A β 42 as shown by a small upfield shift and decreased intensity of the N ^{ϵ} -H ^{ϵ} crosspeak in ¹⁵N–¹H HSQC (Figure 4B). The data suggested that A β (39–42) bound weakly, yet specifically to A β 42 at positions near the charged residues D1, R5, and D7 at the N-terminus, as well as near D23.

To further explore the binding, we studied the interaction of two analogues that showed weak or moderate inhibition of A β 42-induced toxicity (Figure 1) and increase in [Y1]A β 42 fluorescence (Figure 3D and Supporting Information Figure S3), Ac-VVIA and vvia, in NMR binding experiment. The chemical shift changes of D1, D7, and D23 found upon addition of Ac-VVIA (Supporting Information Figure S4) and vvia (inverso-peptide) (Supporting Information Figure S5) were small, similar to those induced by VVIA. These results were consistent with the toxicity inhibition and intrinsic fluorescence data, but the small magnitude of the effects observed in the NMR experiments did not allow drawing further conclusions regarding the binding site(s) of the tetrapeptide derivatives on A β 42.

DISCUSSION AND CONCLUSIONS

A β (39–42) is a promising inhibitor of A β 42-induced toxicity, which unlike most peptide-based drug leads, has favorable physicochemical characteristics. For future development of this peptide lead toward metabolically stable peptidomimetic derivatives, a detailed understanding of its mechanism of action is needed. Here, using a combination of cell cultural and biophysical methods, we found that the major mechanism by which A β (39–42) inhibits A β 42-induced toxicity is through specific interaction with A β 42, in agreement with computer modeling predictions,²⁵ DLS,^{23,24} and ion-mobility-spectroscopy–mass-spectrometry findings.⁴⁰ In addition, A β (39–42) showed a weak, nonspecific protective effect. Interestingly, contrary to our initial hypothesis, the binding of A β (39–42) appears to occur predominantly at the N-terminus of A β 42.

Determination of the binding site of compounds that inhibit A β assembly and toxicity is challenging because of the difficulties associated with high-resolution structural study of A β itself. Co-crystals of A β with inhibitors are difficult to obtain, and the metastable character of A β oligomers does not lend itself easily to high-resolution structure determination. The combination of our SAR (Figure 1), fluorescence (Figure 3), and NMR (Figure 4) data, and the weak effect of A β (39–42) on alamethicine- or α -synuclein-induced toxicity (Figure 2) all suggest that A β (39–42) binds to A β 42 specifically, predominantly at the N-terminus.

Multiple findings support an important role for the N-terminus of A β in mediating assembly and toxicity. Two familial AD-linked mutations resulting in the English (H6R)⁴¹ and Tottori (D7N)⁴² variants were found to stabilize ordered secondary structural elements in A β monomers, facilitate A β oligomerization, and produce oligomeric assemblies that are larger and are more toxic than those of WT A β .⁴³ In addition, a double substitution of the first two N-terminal residues of A β , D1E/A2V, increases protofibril formation substantially.⁴⁴ Thus, the N-terminal region plays an important role in A β assembly and toxicity, suggesting that small molecule binding in this region may inhibit A β toxicity. In addition, N-terminally truncated A β analogues, particularly those containing an N-terminal pyroglutamate (pE), e.g., [pE3]A β or [pE11]A β , were found in senile plaques and have been reported to form β -sheet faster and with higher propensity^{45,46} and to be more toxic than WT A β .^{47,48} One mechanism by which A β (39–42) may reduce A β 42 toxicity is by masking putative enzymatic cleavage sites and thereby preventing the truncation of the N-terminus.

The observation that the N-terminally acetylated A β (39–42) analogues, Ac-VVIA and Ac-AIVV, did not inhibit A β 42-induced toxicity suggests that electrostatic interactions between the unprotected, positively charged N-terminal amino group of A β (39–42) and negatively charged side-chain groups in A β 42 might be important for inhibitory activity. The observation of small chemical shift changes in the resonances of D1 and D7, but not E3 (Figure 4A), supports the specificity of the binding. An alternative explanation for the lack of inhibition by the acetylated peptides may be creation of specific degradation signals (degrons),⁴⁹ leading to rapid proteolysis of Ac-VVIA and Ac-AIVV. However, the large difference between the perturbation of the intrinsic fluorescence of [Y1]A β 42 by free and acetylated analogues (Figure 3D and Supporting Information Figure S3) supports an important role for Coulombic interaction involving the amino group of A β (39–42) and negatively charged side chains in the N-terminus of

*Aβ*42 and suggest that degradation is unlikely the reason for the low inhibition by the acetylated analogues. The observations that amidation of the C-terminus also lowered perturbation of [Y1]*Aβ*42 fluorescence (Figure 3D) and of a chemical shift and intensity change in the resonance of R5 (Figure 4B) provide additional support for contribution of specific electrostatic interactions between *Aβ*(39–42) and the N-terminal region of *Aβ*42.

In addition to the electrostatic interactions found here, modeling studies have suggested that the hydrophobic residues A2 and F4 are important for interaction of *Aβ* with cellular membranes and potential inhibitors.^{25,50} Our data also support an amphiphilic character for the interaction between *Aβ*(39–42) and the N-terminus of *Aβ*42. Thus, the SAR experiments (Figure 1) show that both the hydrophobic side chain at position 41 and the charged N-terminal amino group are important for inhibitory activity.

The C-terminus of *Aβ*42 is predicted to be shielded to a large extent from the aqueous milieu in *Aβ* oligomers, a prediction supported by multiple studies,^{6–8,10,51} and by the high fluorescence of the Y residues in [Y30]*Aβ*42 and [Y42]*Aβ*42 (Figure 3C). Thus, the observation that the fluorescence of [Y30]*Aβ*42 and [Y42]*Aβ*42 did not change significantly upon addition of *Aβ*(39–42) may result from lower accessibility of the C-terminal region of *Aβ*42 to the tetrapeptide. Alternatively, *Aβ*(39–42) may bind the C-terminus without causing substantial change in Y fluorescence because the overall hydrophobicity in the vicinity of the Y side-chain does not change significantly. However, we did not observe any perturbation of NMR resonances in the C-terminal region of *Aβ*42 in the presence of 8-fold molar excess *Aβ*(39–42), suggesting low probability of binding of the tetrapeptide in this region.

Notably, we observed an increase in the fluorescence emission of *Aβ*42 analogues and their mixtures with tetrapeptides in wavelengths longer than the Y emission window (Supporting Information Figure S2). This increase in emission likely is due to light scattering and presumably reflects promotion of *Aβ*42 assembly by the tetrapeptides, as we observed previously in DLS experiments.^{23,24}

Although further work will be required to elucidate the exact binding mode of *Aβ*(39–42) to *Aβ*42, our data demonstrate the specificity of this tetrapeptide as an inhibitor of *Aβ*42-induced toxicity and shed light on the mechanism by which *Aβ*(39–42) binds to *Aβ*42 and blocks its toxicity. The current study provides structural basis for future development of effective and stable peptidomimetic inhibitors of *Aβ*42 neurotoxicity as potential AD therapeutics.

EXPERIMENTAL SECTION

Chemicals and Reagents. 9-Fluorenylmethoxycarbonyl (Fmoc)-protected amino acids and NovaSyn TGA resin were purchased from Novabiochem (Gibbstown, NJ). Wang and PAL resins and all other reagents were obtained from Sigma-Aldrich (St. Louis, MO) and were of the highest purity available. High-purity water (18.2 MΩ) was obtained using a Milli-Q system (Millipore, Bedford, MA).

Peptide Synthesis. Synthesis, purification, and characterization of *Aβ*42 and *Aβ*42 analogues with Y substituted at positions 1, 20, 30, and 42 and F substituted at position 10 were carried out as described previously,³⁴ purified using reverse-phase high-performance liquid chromatography (RP-HPLC), and characterized by MS and amino acid analysis (AAA).

Aβ(39–42) and its derivatives were synthesized using a Discover microwave-assisted synthesis system (CEM, Matthews, NC) using the

following general protocol: Fmoc-protected, preloaded NovaSyn TGA resin or PAL resin (0.1 mmol) was placed in a peptide synthesis vessel, swollen in *N,N*-dimethylformamide (DMF), and deprotected with 5 mL of 20% piperidine (or 4-methylpiperidine) in DMF for 20 min at room temperature. After washing with DMF thrice, a mixed solution of 0.3 mmol Fmoc-AA-OH, 0.3 mmol 2-(1*H*-benzotriazole-1-yl)-1,1,3,3-tetramethyluronium hexafluorophosphate, and 0.6 mmol *N,N*-diisopropylethylamine in 4 mL of DMF was added to the reaction vessel. The coupling reaction was performed using 40 W microwave energy for 8 min at 50 °C. 2,4,6-Trinitrobenzenesulfonic acid test was applied to check for remaining free amino groups.⁵² Coupling efficiency was monitored by the formation of piperidine-dibenzofulvene or 4-methylpiperidine-dibenzofulvene using UV spectroscopy.^{53,54} Acetylation of the N-terminus of Ac-VVIA and Ac-AIVV was performed using acetic anhydride/pyridine (1:2 v/v). After completion of the sequence, the resin was thoroughly washed with DMF and then with dichloromethane, dried under vacuum, and the peptide was cleaved using a mixture of trifluoroacetic acid/1,2-ethanedithiol/H₂O (95:2.5:2.5). Peptides were precipitated by addition of cold diethyl ether and purified by RP-HPLC. The purity of all peptides was higher than 95% determined by analytical RP-HPLC. Peptides were further characterized by MS and AAA. The peptide sequences, calculated masses, and observed masses are listed in Table 2.

Cell Viability Assays. The methods for evaluation of the biological activity of the CTFs themselves and their inhibition of *Aβ*42-induced toxicity were described previously.²³ Briefly, PC-12 cells were differentiated into a neuronal phenotype by incubation with nerve growth factor (100 ng/mL) for 48 h. For initial screening of the new analogues, the cells then were incubated with solutions of *Aβ*42 alone at 10 μM nominal concentration, *Aβ*(39–42) analogues alone at 100 μM nominal concentration, or *Aβ*42:*Aβ*(39–42) analogue mixtures at 1:10 concentration ratio, respectively, for 24 h. Cell viability was determined by the MTT assay using a CellTiter 96 kit (Promega, Madison, WI). Negative controls included NaOH at the same concentration as in the peptide solutions and medium alone. A positive control was 1 μM staurosporine for full kill, which was used to represent a 100% reduction in cell viability, based on which the percentage viability of all of the experimental conditions was calculated.

Active analogues were characterized further in dose–response experiments. In these experiments, *Aβ*42 alone and *Aβ*42:*Aβ*(39–42) analogue mixtures at 1:1, 1:2, 1:5, and 1:10, or 1:1, 1:3 and 1:10, concentration ratios were used and cell viability was determined by both the MTT assay and the LDH-release assay (CytoTox-ONE Homogenous Membrane Integrity Assay kit (Promega)). At least three independent experiments with six replicates ($n \geq 18$) were performed for each assay. The results were averaged and presented as mean \pm SEM. Dose–response assays for inhibition of staurosporine-, α -synuclein-, or alamethicin-induced toxicity by *Aβ*(39–42) were performed using a similar protocol.

Intrinsic Fluorescence. *Aβ*42 or its Y-substituted analogues in the absence or presence of *Aβ*(39–42) or its analogues were treated with HFIP as described previously.⁵⁵ Dry, HFIP-treated peptide films were dissolved in 60 mM NaOH at 10% of the final volume and then diluted with 10 mM sodium phosphate, pH 7.4, to the final nominal concentrations, *Aβ*42 at 5 μM and *Aβ*(39–42) or its analogues at 50 μM. Samples were centrifuged at 5000 *g* for 1 min to remove trace amount of dust particles that could interfere with the experiment due to light scattering. The exact concentration was determined post facto by AAA. Fluorescence was measured using a Hitachi F4500 spectrofluorimeter (Hitachi Instruments, Rye, NH) with excitation at 280 nm and emission in the range 290–400 nm. At least 10 measurements of \sim 1 min each were taken immediately following sample preparation. All fluorescence measurements were carried out at 22 °C with a scan rate of 240 nm/min. Slit widths used for excitation and emission were 5 and 10 nm, respectively. The fluorescence emission spectrum of the phosphate buffer (background intensity) was subtracted from the emission spectrum of each sample. The area under the curve was calculated and normalized as the fluorescence intensity per micromole. Four independent experiments were carried out. The

results were averaged and are presented as mean \pm SEM of fluorescence intensity (arbitrary units) or percentage of the fluorescence intensity of control peptides.

Electron Microscopy. Morphological examination was performed as described briefly.⁵⁶ Briefly, aliquots of each A β 42 analogue in the absence or presence of A β (39–42) or its analogues were spotted on glow-discharged, carbon-coated Formvar grids (Electron Microscopy Science, Hatfield, PA). The samples were the same as those used in the fluorescence experiments. Samples were incubated for 10 min, fixed with 5 μ L 2.5% glutaraldehyde for 10 min, and stained with 5 μ L of 1% uranyl acetate for 10 min. Three to six replicates of each peptide were analyzed using a CX 100 transmission electron microscope (JEOL, Peabody, MA).

Solution-State NMR. Uniformly isotopically labeled A β 42 (15 N] or [13 C/ 15 N]) were purchased from rPeptide (Athens, GA) and treated with HFIP to disaggregate pre-existing aggregates as described previously.⁵⁵ The peptide was dissolved in 20 mM potassium phosphate, pH 7.2, at nominal concentration 1 mg/mL and then sonicated for 1 min. A β (39–42) was dissolved in 10 mM NaOH at 2 mg/mL and sonicated for 1 min. Then, A β 42 and A β (39–42) were mixed slowly to final concentrations 32 and 256 μ M, respectively (1:8 concentration ratio). A control 15 N-A β 42 sample at 32 μ M was prepared by adding the same proportion of buffer and NaOH in the absence of A β (39–42) to the A β 42 stock solution to match the solvent concentration and pH. 2D 15 N– 1 H HSQC NMR spectra of freshly prepared 15 N-labeled A β 42 samples in the absence or presence of A β (39–42) were collected at 4 $^{\circ}$ C using a 600 MHz Bruker Avance II spectrometer equipped with a cryoprobe. The acquisition time was \sim 37 min for each HSQC spectrum. The average intensity percentage of the five strongest, unequivocally assigned peaks in A β 42 (Y10, V18, A21, I32, and L34) was used to calculate the relative A β 42 monomer concentration. H $^{\beta}$ (C $^{\beta}$)CO experiments were collected to support aspartate assignments in A β 42 and to monitor A β 42 and A β (39–42) interactions.

■ ASSOCIATED CONTENT

■ Supporting Information

Dose–response inhibition of A β 42-induced toxicity by A β (39–42) analogues, change in intrinsic fluorescence of each Y-substituted A β 42 analogue upon addition of A β (39–42) and derivatives, fluorescence change of [Y1]A β 42 upon addition of each A β (39–42) derivative, and chemical shift of A β 42 in solution-state, 2D-NMR in the absence and presence of Ac-VVIA or vvIA. This material is available free of charge via the Internet at <http://pubs.acs.org>.

■ AUTHOR INFORMATION

Corresponding Author

*Phone: (310) 206-2082. Fax: (310) 206-1700. E-mail: gbitan@mednet.ucla.edu.

Present Address

[†]Department of Biology, Whittier College, 13406 East Philadelphia Street, Whittier, CA 90608.

■ ACKNOWLEDGMENTS

We thank Dr. David Teplow for the use of his spectrofluorometer and plate reader and Drs. Brigita Urbanc, Raz Jelinek, Farid Rahimi, Inna Solomonov, and Panchanan Maiti for critical reading of the manuscript and helpful discussions. The work was supported by grant AG027818 from the NIH/NIA.

■ ABBREVIATIONS USED

AAA, amino acid analysis; A β , amyloid β -protein; AD, Alzheimer's disease; CHC, central hydrophobic cluster; CTF,

C-terminal fragment; DMF, *N,N*-dimethylformamide; EM, electron microscopy; FMOC, 9-fluorenylmethoxycarbonyl; HFIP, 1,1,1,3,3,3-hexafluoroisopropanol; HSQC, heteronuclear single quantum coherence; LDH, lactate dehydrogenase; MTT, (3-(4,5-dimethylthiazol-2-yl)-2,5-diphenyltetrazolium bromide; MS, mass spectrometry; RP-HPLC, reverse-phase high-performance liquid chromatography; SAR, structure–activity relationship; ST, staurosporine; tPSA, topological polar surface area; WT, wild-type

■ REFERENCES

- (1) Walsh, D. M.; Selkoe, D. J. A β oligomers—a decade of discovery. *J. Neurochem.* **2007**, *101*, 1172–1184.
- (2) Kirkitadze, M. D.; Bitan, G.; Teplow, D. B. Paradigm shifts in Alzheimer's disease and other neurodegenerative disorders: the emerging role of oligomeric assemblies. *J. Neurosci. Res.* **2002**, *69*, 567–577.
- (3) Hardy, J.; Selkoe, D. J. The amyloid hypothesis of Alzheimer's disease: progress and problems on the road to therapeutics. *Science* **2002**, *297*, 353–356.
- (4) Ferreira, S. T.; Vieira, M. N.; De Felice, F. G. Soluble protein oligomers as emerging toxins in Alzheimer's and other amyloid diseases. *IUBMB Life* **2007**, *59*, 332–345.
- (5) Dahlgren, K. N.; Manelli, A. M.; Stine, W. B. Jr.; Baker, L. K.; Krafft, G. A.; LaDu, M. J. Oligomeric and fibrillar species of amyloid- β peptides differentially affect neuronal viability. *J. Biol. Chem.* **2002**, *277*, 32046–32053.
- (6) Bitan, G.; Kirkitadze, M. D.; Lomakin, A.; Vollers, S. S.; Benedek, G. B.; Teplow, D. B. Amyloid β -protein (A β) assembly: A β 40 and A β 42 oligomerize through distinct pathways. *Proc. Natl. Acad. Sci. U.S.A.* **2003**, *100*, 330–335.
- (7) Bernstein, S. L.; Dupuis, N. F.; Lazo, N. D.; Wyttenbach, T.; Condrion, M. M.; Bitan, G.; Teplow, D. B.; Shea, J.-E.; Ruotolo, B. T.; Robinson, C. V.; Bowers, M. T. Amyloid- β protein oligomerization and the importance of tetramers and dodecamers in the aetiology of Alzheimer's disease. *Nature Chem.* **2009**, *1*, 326–331.
- (8) Bitan, G.; Vollers, S. S.; Teplow, D. B. Elucidation of primary structure elements controlling early amyloid β -protein oligomerization. *J. Biol. Chem.* **2003**, *278*, 34882–34889.
- (9) Lazo, N. D.; Grant, M. A.; Condrion, M. C.; Rigby, A. C.; Teplow, D. B. On the nucleation of amyloid β -protein monomer folding. *Protein Sci.* **2005**, *14*, 1581–1596.
- (10) Urbanc, B.; Cruz, L.; Yun, S.; Buldyrev, S. V.; Bitan, G.; Teplow, D. B.; Stanley, H. E. In silico study of amyloid β -protein folding and oligomerization. *Proc. Natl. Acad. Sci. U.S.A.* **2004**, *101*, 17345–17350.
- (11) Tjernberg, L. O.; Näslund, J.; Lindqvist, F.; Johansson, J.; Karlstrom, A. R.; Thyberg, J.; Terenius, L.; Nordstedt, C. Arrest of β -amyloid fibril formation by a pentapeptide ligand. *J. Biol. Chem.* **1996**, *271*, 8545–8548.
- (12) Soto, C.; Kindy, M. S.; Baumann, M.; Frangione, B. Inhibition of Alzheimer's amyloidosis by peptides that prevent β -sheet conformation. *Biochem. Biophys. Res. Commun.* **1996**, *226*, 672–680.
- (13) Lowe, T. L.; Strzelec, A.; Kiessling, L. L.; Murphy, R. M. Structure–function relationships for inhibitors of β -amyloid toxicity containing the recognition sequence KLVFF. *Biochemistry* **2001**, *40*, 7882–7889.
- (14) Findeis, M. A.; Musso, G. M.; Arico-Muendel, C. C.; Benjamin, H. W.; Hundal, A. M.; Lee, J. J.; Chin, J.; Kelley, M.; Wakefield, J.; Hayward, N. J.; Molineaux, S. M. Modified-peptide inhibitors of amyloid β -peptide polymerization. *Biochemistry* **1999**, *38*, 6791–6800.
- (15) Hughes, E.; Burke, R. M.; Doig, A. J. Inhibition of toxicity in the β -amyloid peptide fragment β -(25–35) using *N*-methylated derivatives—a general strategy to prevent amyloid formation. *J. Biol. Chem.* **2000**, *275*, 25109–25115.
- (16) Gordon, D. J.; Sciarretta, K. L.; Meredith, S. C. Inhibition of β -amyloid(40) fibrillogenesis and disassembly of β -amyloid(40) fibrils by short β -amyloid congeners containing *N*-methyl amino acids at alternate residues. *Biochemistry* **2001**, *40*, 8237–8245.

- (17) Zhang, S.; Iwata, K.; Lachenmann, M. J.; Peng, J. W.; Li, S.; Stimson, E. R.; Lu, Y.; Felix, A. M.; Maggio, J. E.; Lee, J. P. The Alzheimer's peptide $A\beta$ adopts a collapsed coil structure in water. *J. Struct. Biol.* **2000**, *130*, 130–141.
- (18) Hochdörffer, K.; März-Berberich, J.; Nagel-Steger, L.; Epple, M.; Meyer-Zaika, W.; Horn, A. H.; Sticht, H.; Sinha, S.; Bitan, G.; Schrader, T. Rational design of β -sheet ligands against $A\beta_{42}$ -induced toxicity. *J. Am. Chem. Soc.* **2011**, *133*, 4348–4358.
- (19) Hetenyi, C.; Szabo, Z.; Klement, T.; Datki, Z.; Kortvelyesi, T.; Zarandi, M.; Penke, B. Pentapeptide amides interfere with the aggregation of β -amyloid peptide of Alzheimer's disease. *Biochem. Biophys. Res. Commun.* **2002**, *292*, 931–936.
- (20) Szegedi, V.; Fülöp, L.; Farkas, T.; Rozsa, E.; Robotka, H.; Kis, Z.; Penke, Z.; Horvath, S.; Molnar, Z.; Datki, Z.; Soos, K.; Toldi, J.; Budai, D.; Zarandi, M.; Penke, B. Pentapeptides derived from $A\beta_{1-42}$ protect neurons from the modulatory effect of $A\beta$ fibrils—an in vitro and in vivo electrophysiological study. *Neurobiol. Dis.* **2005**, *18*, 499–508.
- (21) Pratim Bose, P.; Chatterjee, U.; Nerelius, C.; Govender, T.; Norstrom, T.; Gogoll, A.; Sandegren, A.; Gothelid, E.; Johansson, J.; Arvidsson, P. I. Poly-N-methylated amyloid β -peptide ($A\beta$) C-terminal fragments reduce $A\beta$ toxicity in vitro and in *Drosophila melanogaster*. *J. Med. Chem.* **2009**, *52*, 8002–8009.
- (22) Rahimi, A. F.; Shanmugam, A.; Bitan, G. Structure–function relationships of pre-fibrillar protein assemblies in Alzheimer's disease and related disorders. *Curr. Alzheimer Res.* **2008**, *5*, 319–341.
- (23) Fradinger, E. A.; Monien, B. H.; Urbanc, B.; Lomakin, A.; Tan, M.; Li, H.; Spring, S. M.; Condrón, M. M.; Cruz, L.; Xie, C. W.; Benedek, G. B.; Bitan, G. C-Terminal peptides coassemble into $A\beta_{42}$ oligomers and protect neurons against $A\beta_{42}$ -induced neurotoxicity. *Proc. Natl. Acad. Sci. U.S.A.* **2008**, *105*, 14175–14180.
- (24) Li, H.; Monien, B. H.; Lomakin, A.; Zemel, R.; Fradinger, E. A.; Tan, M.; Spring, S. M.; Urbanc, B.; Xie, C. W.; Benedek, G. B.; Bitan, G. Mechanistic investigation of the inhibition of $A\beta_{42}$ assembly and neurotoxicity by $A\beta_{42}$ C-terminal fragments. *Biochemistry* **2010**, *49*, 6358–6364.
- (25) Urbanc, B.; Betnel, M.; Cruz, L.; Li, H.; Fradinger, E. A.; Monien, B. H.; Bitan, G. Structural basis for $A\beta_{(1-42)}$ toxicity inhibition by $A\beta$ C-terminal fragments: discrete molecular dynamics study. *J. Mol. Biol.* **2011**, *410*, 316–328.
- (26) Lipinski, C. A.; Lombardo, F.; Dominy, B. W.; Feeney, P. J. Experimental and computational approaches to estimate solubility and permeability in drug discovery and development settings. *Adv. Drug Delivery Rev.* **2001**, *46*, 3–26.
- (27) Veber, D. F.; Johnson, S. R.; Cheng, H. Y.; Smith, B. R.; Ward, K. W.; Kopple, K. D. Molecular properties that influence the oral bioavailability of drug candidates. *J. Med. Chem.* **2002**, *45*, 2615–2623.
- (28) Bertrand, R.; Solary, E.; O'Connor, P.; Kohn, K. W.; Pommier, Y. Induction of a common pathway of apoptosis by staurosporine. *Exp. Cell Res.* **1994**, *211*, 314–321.
- (29) Arispe, N.; Diaz, J. C.; Simakova, O. $A\beta$ ion channels. Prospects for treating Alzheimer's disease with $A\beta$ channel blockers. *Biochim. Biophys. Acta* **2007**, *1768*, 1952–1965.
- (30) Sokolov, Y.; Kozak, J. A.; Kaye, R.; Chanturiya, A.; Glabe, C.; Hall, J. E. Soluble amyloid oligomers increase bilayer conductance by altering dielectric structure. *J. Gen. Physiol.* **2006**, *128*, 637–647.
- (31) Fringeli, U. P.; Fringeli, M. Pore formation in lipid membranes by alamethicin. *Proc. Natl. Acad. Sci. U.S.A.* **1979**, *76*, 3852–3856.
- (32) Auluck, P. K.; Caraveo, G.; Lindquist, S. α -Synuclein: membrane interactions and toxicity in Parkinson's disease. *Annu. Rev. Cell Dev. Biol.* **2010**, *26*, 211–233.
- (33) Condrón, M. M.; Monien, B. H.; Bitan, G. Synthesis and purification of highly hydrophobic peptides derived from the C-terminus of amyloid β -protein. *Open Biotechnol. J.* **2008**, *2*, 87–93.
- (34) Maji, S. K.; Amsden, J. J.; Rothschild, K. J.; Condrón, M. M.; Teplow, D. B. Conformational dynamics of amyloid β -protein assembly probed using intrinsic fluorescence. *Biochemistry* **2005**, *44*, 13365–13376.
- (35) Maji, S. K.; Ogorzalek Loo, R. R.; Inayathullah, M.; Spring, S. M.; Vollers, S. S.; Condrón, M. M.; Bitan, G.; Loo, J. A.; Teplow, D. B. Amino acid position-specific contributions to amyloid β -protein oligomerization. *J. Biol. Chem.* **2009**, *284*, 23580–23591.
- (36) Lakowicz, J. R. *Principles of Fluorescence Spectroscopy*; 2nd ed.; Kluwer Academic/Plenum Publishers: New York, 1999; p 698.
- (37) Zagorski, M. G.; Yang, J.; Shao, H.; Ma, K.; Zeng, H.; Hong, A. Methodological and chemical factors affecting amyloid β peptide amyloidogenicity. *Methods Enzymol.* **1999**, *309*, 189–204.
- (38) Stine, W. B. Jr.; Dahlgren, K. N.; Krafft, G. A.; LaDu, M. J. In vitro characterization of conditions for amyloid- β peptide oligomerization and fibrillogenesis. *J. Biol. Chem.* **2003**, *278*, 11612–11622.
- (39) Yan, Y.; Wang, C. $A\beta_{42}$ is more rigid than $A\beta_{40}$ at the C terminus: implications for $A\beta$ aggregation and toxicity. *J. Mol. Biol.* **2006**, *364*, 853–862.
- (40) Gessel, M. M.; Wu, C.; Li, H.; Bitan, G.; Shea, J. E.; Bowers, M. T. Unpublished results.
- (41) Janssen, J. C.; Beck, J. A.; Campbell, T. A.; Dickinson, A.; Fox, N. C.; Harvey, R. J.; Houlden, H.; Rossor, M. N.; Collinge, J. Early onset familial Alzheimer's disease—mutation frequency in 31 families. *Neurology* **2003**, *60*, 235–239.
- (42) Wakutani, Y.; Watanabe, K.; Adachi, Y.; Wada-Isoe, K.; Urakami, K.; Ninomiya, H.; Saido, T. C.; Hashimoto, T.; Iwatsubo, T.; Nakashima, K. Novel amyloid precursor protein gene missense mutation (D678N) in probable familial Alzheimer's disease. *J. Neurol. Neurosurg. Psychiatry* **2004**, *75*, 1039–1042.
- (43) Ono, K.; Condrón, M. M.; Teplow, D. B. Effects of the English (H6R) and Tottori (D7N) familial Alzheimer disease mutations on amyloid β -protein assembly and toxicity. *J. Biol. Chem.* **2010**, *285*, 23186–23197.
- (44) Qahwash, I.; Weiland, K. L.; Lu, Y. F.; Sarver, R. W.; Kletzien, R. F.; Yan, R. Q. Identification of a mutant amyloid peptide that predominantly forms neurotoxic protofibrillar aggregates. *J. Biol. Chem.* **2003**, *278*, 23187–23195.
- (45) He, W. L.; Barrow, C. J. The $A\beta$ 3-pyroglytamy and 11-pyroglytamy peptides found in senile plaque have greater β -sheet forming and aggregation propensities in vitro than full-length $A\beta$. *Biochemistry* **1999**, *38*, 10871–10877.
- (46) Schilling, S.; Lauber, T.; Schaupp, M.; Manhart, S.; Scheel, E.; Böhm, G.; Demuth, H. U. On the seeding and oligomerization of pGlu-amyloid peptides (in vitro). *Biochemistry* **2006**, *45*, 12393–12399.
- (47) Russo, C.; Violani, E.; Salis, S.; Venezia, V.; Dolcini, V.; Damonte, G.; Benatti, U.; D'Arrigo, C.; Patrone, E.; Carlo, P.; Schettini, G. Pyroglutamate-modified amyloid β -peptides— $A\beta$ N3(pE)-strongly affect cultured neuron and astrocyte survival. *J. Neurochem.* **2002**, *82*, 1480–1489.
- (48) Wirths, O.; Breyhan, H.; Cynis, H.; Schilling, S.; Demuth, H. U.; Bayer, T. A. Intraneuronal pyroglutamate- $A\beta$ 3–42 triggers neurodegeneration and lethal neurological deficits in a transgenic mouse model. *Acta Neuropathol.* **2009**, *118*, 487–496.
- (49) Hwang, C. S.; Shemorry, A.; Varshavsky, A. N-Terminal acetylation of cellular proteins creates specific degradation signals. *Science* **2010**, *327*, 973–977.
- (50) Urbanc, B.; Betnel, M.; Cruz, L.; Bitan, G.; Teplow, D. B. Elucidation of amyloid β -protein oligomerization mechanisms: discrete molecular dynamics study. *J. Am. Chem. Soc.* **2010**, *132*, 4266–4280.
- (51) Zhao, W. Q.; Toolan, D.; Hepler, R. W.; Wolfe, A. L.; Yu, Y.; Price, E.; Uebele, V. N.; Schachter, J. B.; Reynolds, I. J.; Renger, J. J.; McCampbell, A.; Ray, W. J. High throughput monitoring of amyloid- β_{42} assembly into soluble oligomers achieved by sensitive conformation state-dependent immunoassays. *J. Alzheimer's Dis.* **2011**, *25*, 655–669.
- (52) Chan, W. C.; White, P. D. *Fmoc Solid-Phase Peptide Synthesis: A Practical Approach*; Oxford University Press: New York, 2000; p xxiv, 346.

(53) Gude, M.; Ryf, J.; White, P. D. An accurate method for the quantitation of Fmoc-derivatized solid phase support. *Letts. Pept. Sci.* **2002**, *9*, 203–206.

(54) Varady, L.; Rajur, S. B.; Nicewonger, R. B.; Guo, M.; Ditto, L. Fast and quantitative high-performance liquid chromatography method for the determination of 9-fluorenylmethoxycarbonyl release from solid-phase synthesis resins. *J. Chromatogr., A* **2000**, *869*, 171–179.

(55) Rahimi, F.; Maiti, P.; Bitan, G. Photo-induced cross-linking of unmodified proteins (PICUP) applied to amyloidogenic peptides. *J. Vis. Exp.* **2009**, <http://www.jove.com/index/details.stp?id=1071>.

(56) Li, H.; Monien, B. H.; Fradinger, E. A.; Urbanc, B.; Bitan, G. Biophysical characterization of A β 42 C-terminal fragments: inhibitors of A β 42 neurotoxicity. *Biochemistry* **2010**, *49*, 1259–1267.